

Identification of coexistent load and damage

Qingxia Zhang · Łukasz Jankowski · Zhongdong Duan

Structural and Multidisciplinary Optimization, **41**(2), 2010, pp. 243–253, DOI 10.1007/s00158-009-0421-1.
The original publication is available at <http://www.springerlink.com/content/w2122k110x142168/>
Received: 4 November 2008 / Revised: 12 March 2009 / Accepted: 13 July 2009 / Published online: 7 August 2009

Abstract Load reconstruction and damage identification are crucial problems in structural health monitoring. However, it seems there is not much investigation on identification of coexistent load and damage, although in practice they usually exist together. This paper presents a methodology to solve this problem based on the Virtual Distortion Method. A damaged structure is modeled by an equivalent intact structure subjected to the same loads and to virtual distortions which model the damages. The measured structural response is used to identify the loads, the distortions and to recover the stress-strain relationship of the damaged elements. This way both the damage type and extent are identified. The approach can be used off-line and online by repetitive applications in a moving time window. A numerical experiment of a truss with 5% measurement error validates that the two tested damage types (constant stiffness reduction and breathing crack) can be identified along with the loads.

Keywords Structural health monitoring · Load identification · Damage identification · Virtual Distortion Method (VDM)

Q. Zhang
School of Civil Engineering, Harbin Institute of Technology, P.O. Box 2546, 202 Haihe Road, Harbin 150090, China.
Present address: Smart-Tech Centre, Institute of Fundamental Technological Research, Polish Academy of Sciences, Pawińskiego 5b, 02-106, Warsaw, Poland.
E-mail: mzhang@ippt.gov.pl

Ł. Jankowski (Corresponding author)
Smart-Tech Centre, Institute of Fundamental Technological Research, Polish Academy of Sciences, Pawińskiego 5b, 02-106, Warsaw, Poland.
E-mail: lukasz.jankowski@ippt.gov.pl

Z. Duan
School of Civil Engineering, Harbin Institute of Technology, P.O. Box 2546, 202 Haihe Road, Harbin 150090, China.
E-mail: duanzd@hit.edu.cn

1 Introduction

Identification of coexistent load and damage refers to the simultaneous reconstruction of an unknown external load and damage (both type and size) of a damaged structure. Accurate knowledge of external loads and structural damage is crucial for maintaining safety and integrity of monitored structures as well as for applications in forensic engineering. In recent years, both load and damage identifications have become widely researched topics with several effective methods focusing on either one of them. However, in real applications, unknown damage and unknown loads usually coexist and together influence the system response; the damage can even progress with the external load. Though, identification of coexistent load and damage seems to be an unexplored area.

Relatively recent reviews of the techniques used for off-line *load reconstruction* can be found in Inoue et al (2001); Jacquelin et al (2003) and Uhl (2007). The most often used approaches are model-based, operate in the time domain (Adams and Doyle 2002; Jankowski 2009), frequency domain (Ödéan and Lundberg 1991; Inoue et al 1991) or sometimes wavelet domain (Doyle 1997) and basically reduce the reconstruction to the problem of off-line deconvolution of the measured structural response and the impulse response function which is estimated in advance. For online load identification, observer techniques of unknown input estimation (Ha and Trinh 2004; Klinkov and Fritzen 2006), Kalman filter (Liu et al 2000) as well as the Inverse Structural Filter (ISF) (Allen and Carne 2006, 2008) have been used. The great majority of these methods take into account only linear systems; the relatively few papers that consider nonlinear (Ha and Trinh 2004; Ma and Ho 2004) or elastoplastic (Jankowski 2009) structures assume the model of the nonlinearity to be exactly known in advance. All these methods require thus a precalibrated model of the monitored struc-

ture with well-determined structural parameters, and seem infeasible for load identification in systems with unknown damages. Even if purely experimental data are used to build the impulse response function, as in Suwała and Jankowski (2008), the measured structure is assumed to be intact. Another group of load identification methods is based on computational intelligence techniques. Mujica et al (2006) use case-based reasoning for identification of the location of an impact on an aircraft wing, while Briggs and Tse (1992) use a similar technique to identify both impact location and magnitude. Cao et al (1998) identify static loads acting on an aircraft wing using an artificial neural networks. In general, these and similar methods belong to the class of pattern recognition methods and, in order to build initially the learning load-response patterns, also require a definite structure that remains undamaged.

Damage identification is the primary task of structural health monitoring (SHM) systems. In general, there are two fundamental groups of methods: high- and low-frequency. High-frequency methods are used for local detection and precise identification of defects in a narrow inspection zone, see Silva et al (2008) for a time series approach or Staszewski (2003) for ultrasonic testing. These methods do not require structural modeling and are outside the scope of this paper. Low-frequency methods are aimed at the identification of significant defects in a non-local inspection zone, which is often the whole structure. A vast number of existing approaches can be categorized with respect to various criteria. Holnicki-Szulc (2008) differentiates between model-based and pattern matching approaches, a comparison of two specific methods can be found in Kołakowski et al (2006). Yan (2006) singles out the three general approaches as: (1) modal methods, (2) time domain methods and (3) wavelet methods. The modal methods detect, locate and identify damages by the changes of the related modal parameters; see a summary review in Doebling et al (1998). The time domain methods utilize either statistical concepts and time series models (Nair et al 2006; Wei et al 2005) or deterministic model-updating approaches, which are often coupled with quick reanalysis techniques (Kołakowski et al 2008). The wavelet analysis is usually used with pattern recognition methods (Mujica et al 2005). A part of all these methods rely on the assumption that the external loads are well-defined and known. Others (like some modal and time series methods) can be used without exact information about the loads, but they are still confined to special conditions like ambient excitation or free response of the monitored structure.

Therefore, in the case of coexistent load and damage, the related identification problems are inherently coupled: it is in general not possible to identify the unknown load independently from the unknown damage. This paper proposes a new and effective methodology for simultaneous identification. It is based on the Virtual Distortion Method (VDM)

(Holnicki-Szulc 2008; Holnicki-Szulc and Gierliński 1995) and models the damaged structure by an equivalent intact structure (called *distorted structure*), which is subjected to the same unknown load and certain virtual distortions that model the damage. Both the load and the distortions are reconstructed off-line or online (in a moving time window) using the measured response. The computed distortions are then used to recover the stress-strain relationships of the damaged elements, which allows their damage type and extent to be identified.

The next section reviews briefly the VDM-related concepts that are relevant to the considered problem. The third section discusses the methodology in the case of off-line identification, which is generalized to the online case in the fourth section. The numerical example of the last section tests the methodology with two stiffness-related damage types (constant change of Young's modulus and a breathing crack); their types and extents are successfully estimated at the assumed Gaussian measurement error level of 5% rms.

2 Virtual Distortion Method (VDM)

The Virtual Distortion Method is a quick reanalysis method (Akgün et al 2001), applicable in both statics and dynamics (Holnicki-Szulc 2008; Kołakowski et al 2008). The method expresses the structural response of a *damaged structure* to an external load in the form of a combination of the linear responses of the intact structure to the same load and to certain virtual distortions that occur in the damaged elements (*distorted structure*). Both structures are equivalent in terms of identical element strains and element forces. A virtual distortion models the damage of an element and can be identified with an additionally introduced strain; in the case of a truss element and a stiffness-related damage it is modeled by a pair of self-equilibrated forces which are applied axially at the nodes of the concerned element so that in the static case it would be respectively elastically strained. In the dynamic case the distortions and the corresponding forces are time-dependent.

For the sake of notational simplicity only truss structures, stiffness-related damages and strain sensors are considered in this paper. Nevertheless, these simplifications are inessential, since the methodology can be straightforwardly extended to include other damage patterns as well as types of structures and sensors. The generalizations to plates and frames are discussed in Holnicki-Szulc and Gierliński (1995) and Putresza and Kołakowski (2001). Damages related to element masses can be modeled and identified in a similar way via the related virtual forces, see Holnicki-Szulc (2008) or Wikło and Holnicki-Szulc (2009a). Finally, strain response is chosen here as notationally convenient, because of its straightforward relation to the virtual distortions, see (5b) below.

2.1 Response of a damaged structure to a known load

With the assumption of zero initial conditions, the discretized response $\varepsilon_\alpha(t)$ of the α th element in an externally loaded damaged truss structure is modeled using the VDM as the following sum of the linear and the residual parts:

$$\begin{aligned}\varepsilon_\alpha(t) &= \varepsilon_\alpha^L(t) + \varepsilon_\alpha^R(t) \\ &= \varepsilon_\alpha^L(t) + \sum_{\tau=0}^t \sum_{\beta} D_{\alpha\beta}^\varepsilon(t-\tau) \varepsilon_\beta^0(\tau),\end{aligned}\quad (1)$$

where $\varepsilon_\alpha^L(t)$ denotes the linear response of the intact structure to the same load, $\varepsilon_\beta^0(t)$ is the virtual distortion in the β th damaged element and $D_{\alpha\beta}^\varepsilon(t)$ is the discretized system transfer function (*dynamic influence matrix* according to the VDM terminology), which is the discretized strain response of the α th element of the intact structure to an impulse virtual distortion in the β th element. Here and henceforth, the summations indexed by α or β extend over all potentially damaged elements. Note that this formulation requires the assumption of *small deformations* in order to allow the responses to be linearly combined. In modeling the stresses of the damaged elements, the virtual distortion has to be subtracted from the total strain,

$$\sigma_\alpha(t) = E_\alpha [\varepsilon_\alpha(t) - \varepsilon_\alpha^0(t)], \quad (2)$$

where E_α denotes the original Young's modulus of the undamaged α th element.

2.2 Virtual distortions vs. damage

The virtual distortion $\varepsilon_\alpha^0(t)$ occurs in the α th element and models its stiffness-related defect, which is expressed in terms of the (possibly time-dependent) modified effective stiffness $\widehat{E}_\alpha(t)$ or the corresponding stiffness modification coefficient $\mu_\alpha(t)$,

$$\mu_\alpha(t) = \frac{\widehat{E}_\alpha(t)}{E_\alpha}. \quad (3)$$

The distortion can be related to the stiffness modification coefficient by the already mentioned postulate of the equality of the element forces,

$$\begin{aligned}\widehat{f}_\alpha(t) &= \widehat{E}_\alpha(t) A_\alpha \varepsilon_\alpha(t), \\ f_\alpha(t) &= A_\alpha \sigma_\alpha(t) = A_\alpha E_\alpha [\varepsilon_\alpha(t) - \varepsilon_\alpha^0(t)],\end{aligned}\quad (4)$$

in the damaged and distorted structures, respectively. In (4), A_α denotes the cross-sectional area of the α th element and is assumed to be invariant (otherwise the response is influenced by the respective change of mass, which has to be

modeled by virtual forces, see Holnicki-Szulc (2008)). The force equality requirement yields

$$\mu_\alpha(t) = \frac{\varepsilon_\alpha(t) - \varepsilon_\alpha^0(t)}{\varepsilon_\alpha(t)}, \quad (5a)$$

which is equivalent to

$$\varepsilon_\alpha^0(t) = [1 - \mu_\alpha(t)] \varepsilon_\alpha(t). \quad (5b)$$

Given identified distortions and strains, the actual stiffness modification coefficient $\mu_\alpha(t)$ can be directly computed by (5a). Conversely, if $\mu_\alpha(t)$ is given a priori, as in a numerical simulation of the response, then in order to determine the corresponding virtual distortion, the strain relation (1) has to be substituted into the right-hand side of (5b), which yields

$$\begin{aligned}\sum_{\beta} [\delta_{\alpha\beta} - [1 - \mu_\alpha(t)] D_{\alpha\beta}^\varepsilon(t)] \varepsilon_\beta^0(t) \\ = [1 - \mu_\alpha(t)] \left[\varepsilon_\alpha^L(t) + \sum_{\tau=0}^{t-\Delta t} \sum_{\beta} D_{\alpha\beta}^\varepsilon(t-\tau) \varepsilon_\beta^0(\tau) \right],\end{aligned}\quad (6)$$

where $\delta_{\alpha\beta}$ denotes Kronecker's delta. Equation 6 is a system of linear equations, which should be solved iteratively in the successive time steps. Note that in the case of a non-constant stiffness modification (e.g. a breathing crack with two different values of stiffness used in tension and in compression), the coefficient $\mu_\alpha(t)$ can depend on the actual value of the strain $\varepsilon_\alpha(t)$, so that (6) cannot be used directly. In such a case, the proper values of $\mu_\alpha(t)$ should be determined (possibly iteratively) by

1. taking a *trial step* using the previously determined values $\mu_\alpha(t) := \mu_\alpha(t - \Delta t)$,
2. verifying compliance of the computed strains with the assumed values of $\mu_\alpha(t)$ and,
3. if necessary, updating them and repeating the computations.

A similar procedure is used in Wikło and Holnicki-Szulc (2009b); Jankowski (2009) in the related case of a plastically yielding element and a bilinear constitutive law.

3 Off-line identification

In this section, the initial conditions are assumed to be zero, which makes (1) valid. The case of known nonzero initial conditions is discussed in the next section.

3.1 Response of a damaged structure to an unknown load

According to (1), the response of a damaged structure is a combination of the original linear response of the undamaged structure and of its responses to the virtual distortions, which model the damage. The linear response depends on the unknown load, which has to be identified. Therefore, the response of the damaged structure can be expressed directly in terms of the unknowns of both types as

$$\boldsymbol{\varepsilon}_\alpha(t) = \sum_{\tau=0}^t \sum_i D_{\alpha i}^p(t-\tau) p_i(\tau) + \sum_{\tau=0}^t \sum_\beta D_{\alpha\beta}^e(t-\tau) \boldsymbol{\varepsilon}_\beta^0(\tau), \quad (7)$$

where $p_i(t)$ is the unknown discretized load in the i th potentially load-exposed degree of freedom (DOF) and $D_{\alpha i}^p(t)$ denotes the discretized strain response in the α th element of the intact structure to an impulse force in the i th DOF. Here and henceforth, the i -indexed summation extends over all load-exposed DOFs. Equation 7, rewritten for all considered time steps t and for all sensor locations α , can be stated in the form of a single large linear equation as

$$\boldsymbol{\varepsilon} = \mathbf{D}^p \mathbf{p} + \mathbf{D}^e \boldsymbol{\varepsilon}^0 = [\mathbf{D}^p \ \mathbf{D}^e] \begin{bmatrix} \mathbf{p} \\ \boldsymbol{\varepsilon}^0 \end{bmatrix} = \mathbf{D} \mathbf{z}, \quad (8)$$

where the vector \mathbf{z} collects together the vectors \mathbf{p} and $\boldsymbol{\varepsilon}^0$, which contain respectively all discretized loads in all potentially load-exposed DOFs and all discretized virtual distortions in all damaged elements. The corresponding system transfer matrices are denoted by \mathbf{D} , \mathbf{D}^e and \mathbf{D}^p . By a proper ordering of the elements of \mathbf{z} , the matrix \mathbf{D} can take the rearranged form of a large block matrix composed of Toeplitz matrices, which relate discretized sensor responses to unit excitations and to unit distortions, see an example in Figure 2.

3.2 Identification of load and virtual distortions

According to (7) or (8), information about the unknown load and damage is reflected in the response. The identification amounts basically to the comparison of the computed response $\boldsymbol{\varepsilon}$ to the measured response $\boldsymbol{\varepsilon}^M$ in order to solve the resulting equation,

$$\boldsymbol{\varepsilon}^M = \mathbf{D} \mathbf{z}, \quad (9a)$$

which is a large linear system. To guarantee the uniqueness of the solution, there should be at least as many independent sensors as the total number of potentially load-exposed DOFs and damaged elements. In practice, it requires previous information on the potential locations of the damages and loads. Equation 9 can be solved quickly e.g. by the conjugate gradient method (Dahlquist and Björck 2008; Nocedal and Wright 1999).

3.2.1 Numerical remarks

The system (9a) is dense, and the numbers of equations and unknowns are both proportional to the number of time steps: If the total number of load-exposed DOFs and damages is n_z , the number of sensors is n_s and n_t time steps are considered, then the dimension of \mathbf{D} is $n_s n_t \times n_z n_t$. Hence, in the cases of a dense time discretization or a longer sampling time, the system can become prohibitively large and thus computationally hardly manageable. To reduce the numerical costs, one can utilize the piecewise continuity of distortions and loads. In practice, the time discretization is chosen to be dense enough so that a force or a virtual distortion does not change rapidly and can be effectively approximated e.g. by splines, wavelets or load shape functions (Zhang et al 2008). Equation 9a takes then the following form:

$$\boldsymbol{\varepsilon}^M \approx \mathbf{D} \mathbf{N} \boldsymbol{\alpha}, \quad (9b)$$

where $\mathbf{z} \approx \mathbf{N} \boldsymbol{\alpha}$ and the approximating unknowns $\boldsymbol{\alpha}$ are far fewer in number than the original unknowns \mathbf{z} .

In practical situations, the linear system (9) tends to be ill-conditioned, hence a small disturbance of $\boldsymbol{\varepsilon}^M$ (e.g. an inevitable measurement error) may cause a large error in the identified loads and distortions. In most of the cases the ill-conditioning is inherent and can be attributed to the fact that compact integral operators of the first kind cannot have a bounded inverse (Kress 1989). As an apparently contradictory result, the finer the time discretization, the worse the ill-conditioning. Therefore, it is necessary to numerically regularize the solution; common techniques are the truncated singular value decomposition (TSVD) or the Tikhonov method, see Jacquelin et al (2003); Hansen (2002) or Kress (1989).

3.3 Damage identification

The distortions and the load, identified by (9), can be used by (7) and (2) to recover the stress-strain relationship in the damaged elements and to identify the damage type and extent. In this paper, two types of damages are considered, both expressible in terms of a single stiffness reduction coefficient:

- Constant reduction of stiffness (e.g. related to corrosion),

$$\mu_\alpha(t) = \mu_\alpha^{\text{crs}} < 1. \quad (10a)$$

- Breathing crack model with a reduced stiffness value used in tension,

$$\mu_\alpha(t) = \begin{cases} 1 & \text{if } \varepsilon_\alpha(t) < 0 \text{ (compression),} \\ \mu_\alpha^{\text{bc}} & \text{if } \varepsilon_\alpha(t) \geq 0 \text{ (tension),} \end{cases} \quad (10b)$$

where $\mu_\alpha^{\text{bc}} < 1$. Such a model, although simple, is adequate for low-frequency structural health monitoring (Friswell and Penny 2002).

Other types of stiffness-related phenomena, like buckling, can be treated in a similar way.

For each potentially damaged element, the stress-strain relationship is recovered in the form of a time sequence of pairs $(\varepsilon_\alpha(t), \sigma_\alpha(t))$. Given these pairs, the extent of the damage can be identified by square best-fitting of the theoretical curves separately for each considered damage type,

$$\begin{aligned}\mu_\alpha^{\text{crs}} &= \frac{1}{E_\alpha} \frac{\sum_t \varepsilon_\alpha(t) \sigma_\alpha(t)}{\sum_t \varepsilon_\alpha^2(t)}, \\ \mu_\alpha^{\text{bc}} &= \frac{1}{E_\alpha} \frac{\sum_t \varepsilon_\alpha(t) \sigma_\alpha(t)}{\sum_t \varepsilon_\alpha^2(t)} \mathbb{1}_{\varepsilon_\alpha(t) > 0},\end{aligned}\quad (11)$$

and choosing the damage type that fits the stress-strain relationship better, i.e. minimizes the least-square distance

$$\frac{\sum_t [\sigma_\alpha(t) - \mu_\alpha(t) E_\alpha \varepsilon_\alpha(t)]^2}{\sum_t \sigma_\alpha^2(t)} \quad (12)$$

where $\mu_\alpha(t)$ is defined by (10).

4 Online identification

The main task of identifying the coexistent external load and damage is to solve (9), which is basically a discretized deconvolution problem. The quality of the solution and the computational effort depend mainly on the matrix \mathbf{D} or, for (9b), \mathbf{DN} . When the sampling time is long, both these matrices can be prohibitively large, and each direct solution will be time-consuming and prone to numerical errors. Moreover, (9) can be used only for off-line identification. Therefore, repetitive identification in a moving time window is proposed here in order to eliminate the drawbacks and to enable the online identification. The method utilizes the superposition theorem of linear elastic structures.

4.1 Response of a damaged structure

The damaged structure, including the nonlinear case of a breathing crack, is converted by the VDM into a linear distorted structure. This is indicated by (7), which assumes zero initial conditions. Let the sampling time interval be divided into several possibly overlapping time sections. The response of the distorted structure in the n th section can be expressed by the following modified version of (7):

$$\begin{aligned}\varepsilon_\alpha^{(n)}(t) &= \bar{\varepsilon}_\alpha^{(n)}(t) + \sum_{\tau=0}^t \sum_i D_{\alpha i}^p(t-\tau) p_i^{(n)}(\tau) \\ &\quad + \sum_{\tau=0}^t \sum_\beta D_{\alpha\beta}^\varepsilon(t-\tau) \varepsilon_\beta^{0(n)}(\tau),\end{aligned}\quad (13)$$

which takes into account also the free vibrations $\bar{\varepsilon}_\alpha^{(n)}(t)$ of the undamaged structure caused by the nonzero initial conditions at the beginning of the section. The index (n) denotes the number of the section.

4.2 Identification

The strains computed by Equation 13 can be compared to the measured strains and stated in the form of a single linear equation similar to (9),

$$\boldsymbol{\varepsilon}^{\text{M}(n)} - \bar{\boldsymbol{\varepsilon}}^{(n)} = \mathbf{B}^{(n)} \mathbf{z}^{(n)}, \quad (14)$$

where $\mathbf{B}^{(n)}$ is the matrix \mathbf{D} (or, using approximations, \mathbf{DN}) reduced according to the length of the n th section. Equation 14 covers only one time section and is thus much smaller and easier to solve than (9).

The initial conditions of each time section and the corresponding free vibrations can be computed straightforwardly, provided the loads and the virtual distortions in the previous sections are already identified. Equation 14 can be thus used online, in successive time sections, to obtain iteratively all the unknown loads and virtual distortions in the whole considered time interval.

As observed in practice, the identified loads tend to drift away from the exact solution, which causes a lower accuracy near the end of the time section. A practical way to improve the accuracy is to consider partly overlapping time sections, so that less accurate results from the previous section can be improved in the next time section.

5 Numerical example

5.1 Structure

Figure 1 shows the modeled truss structure. It is 2.5 m long, the elements are 10 mm² in cross-section, 0.5 m or 0.5√2 m long, and made of steel with density 7800 kg/m³ and Young's modulus 210 GPa. Each node weighs 0.13 kg. The two left hand side corner nodes of the bottom plane are deprived all DOFs, while the two opposite right hand side corner nodes are deprived of the vertical DOFs and are free to move in the horizontal plane only.

It is assumed that the structure is loaded by a vertical moving force, which (as indicated in Figure 1) is transferred to the upper five nodes of the structure via a system of rigid beams. Two damages are assumed to occur in the elements no. 21 and 32, and are marked by the dashed lines. Seven sensors are placed on elements no. 1, 4, 15, 17, 21, 23 and 24, which are marked by shorter parallel solid lines. The total considered time interval is $T = 48$ ms, and has been discretized into 240 time steps of $\Delta t = 0.2$ ms each. The full system transfer matrix \mathbf{D} is hence 1687×1687 in dimension. It has been generated numerically using the Newmark integration scheme. Figure 2 illustrates schematically the structure of the matrix: block rows correspond to the sensors, first five block columns to the potentially load-exposed DOFs, last two block columns to the damaged elements and since

Fig. 1 Truss structure modelled in the numerical example

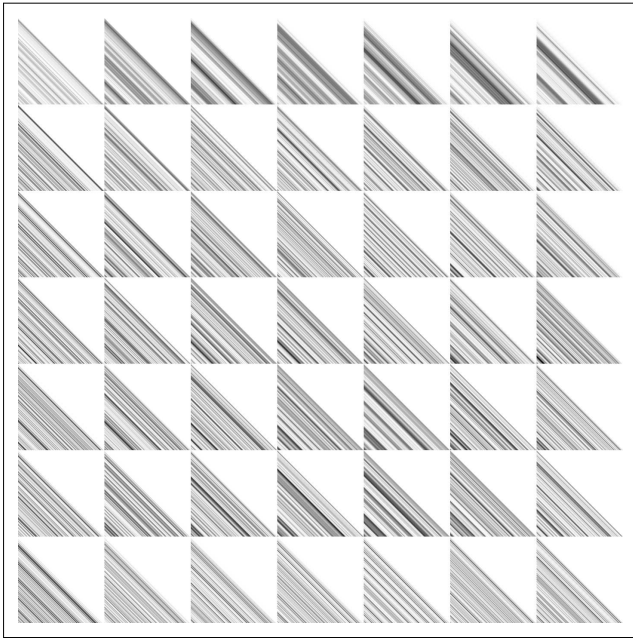
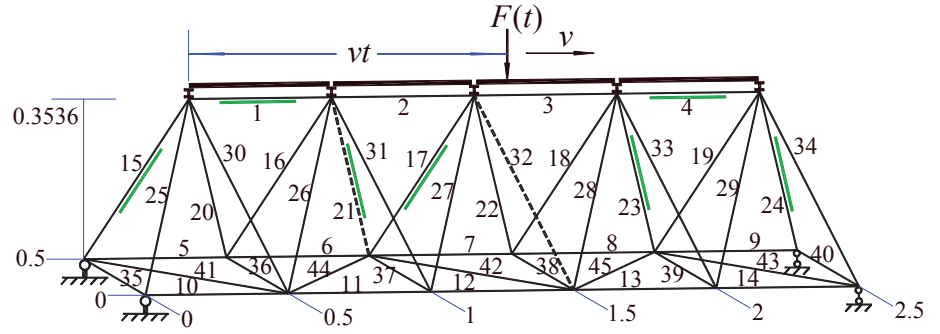


Fig. 2 Structure of the full system transfer matrix \mathbf{D}

there are a total of 240 time steps, each block is a 241×241 lower triangular Toeplitz matrix.

5.2 Actual load and damages

Figure 3 (top left) depicts the evolution of the assumed actual load, which is to be identified in the following with the discussed approaches. The load simulates a time-dependent force moving at a constant velocity 41.667 m/s along the structure. The top right figure plots the corresponding nodal loads. The computed exact responses of the considered strain sensors in the case of the undamaged structure are plotted in the bottom left figure. In order to test the damage identification, two damage types have been considered:

1. Constant stiffness reduction (csr) in the element no. 32: Young's modulus is reduced by 70%,

$$\mu_{32}(t) = 0.3.$$

Table 1 Dimensions of the linear systems (9)

	off-line case	online case
full (\mathbf{D})	1687×1687	847×847
approximated (\mathbf{DN})	1687×126	847×98

2. Breathing 40% crack (bc) in the element no. 21: Young's modulus is reduced when the element is in tension,

$$\mu_{21}(t) = \begin{cases} 1 & \text{if } \varepsilon_{21}(t) \leq 0, \\ 0.6 & \text{if } \varepsilon_{21}(t) > 0. \end{cases}$$

The computed exact response of the corresponding damaged structure is plotted in Figure 3 (bottom right). The response has been contaminated with numerically generated uncorrelated Gaussian noise at the 5% rms level, which simulates the measurement error. By comparison with the response of the undamaged structure (bottom left figure) note the relatively small influence of the considered damages.

5.3 Identification

Both online and off-line identification schemes have been tested. For the online identification, the time interval of the total length of 240 time steps (48 ms) has been divided into three sections of 120 time steps with the overlapping parts of 60 time steps. The identification by (9b) has been also performed with both loads and distortions approximated by the load shape functions, which are constructed from standard shape functions of a frame element (Zhang et al 2008). In the off-line case eighteen approximating functions have been used, while in the online case for each of the three sections fourteen functions have been used. Table 1 lists the dimensions of the resulting matrices \mathbf{D} or \mathbf{DN} of the linear systems (9).

Since the system matrices can be ill-conditioned, TSVD-regularized solutions have been computed. The regularization level has been defined by the number k of the truncated singular values, which in each case has been determined using the L-curve technique, that is by weighting in the log-log scale the residual against the norm of the first differences of the solution, see e.g. Jacquelin et al (2003). In the

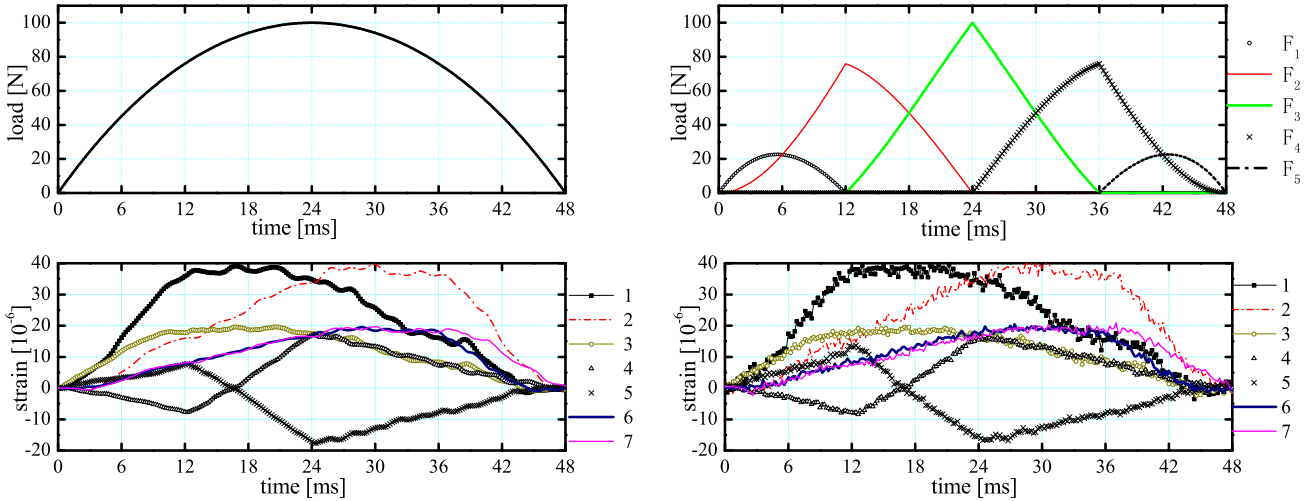


Fig. 3 Assumed actual load and the corresponding computed exact responses of the seven considered strain sensors: (top left) Assumed actual load; (top right) Corresponding equivalent nodal loads; (bottom left) Response of the undamaged structure; (bottom right) Response of the damaged structure contaminated with 5% rms Gaussian measurement error

full off-line case, the corner of the L-curve corresponds to $k \approx 350$, see Figure 4 (left). It has been hence assumed that $k = 357$, that is all singular values less than 0.1% of the maximum singular value have been discarded. For the full online case $k = 194$ has been chosen in a similar way, which corresponds to the singular value truncation level of 0.2%. The L-curves corresponding to the approximated cases, shown in Figure 4 (right) for the off-line case, consist of only the lower branches, which testifies the well-conditioning of the approximated problems. Here a low value of $k = 5$ has been chosen to guarantee the reliability.

Note that the computational cost of a single identification depends mainly on the singular value decomposition (SVD) of the system matrix, which for an $m \times n$ matrix ($m \geq n$) is of order $O(mn^2)$ (Dahlquist and Björck 2008). Hence, as seen in Table 1, the cost can be significantly reduced (almost two orders of magnitude) by using the approximations. The reduction due to the repetitive smaller identifications in the online case, which use the same system matrix and hence require only single decomposition, is less pronounced (below one order of magnitude). In the case of several repetitive identifications, both off-line and online, the numerically costly SVD has to be computed only once, and thus the total cost of a single identification is smaller by one order of magnitude.

5.3.1 Load identification

The actual equivalent nodal loads and the loads identified in the four considered cases are compared in Figure 5. If it is known (or told from the characteristic orderliness of the results) that the loads correspond to a moving load, then the actual moving force can be also constructed; the results are

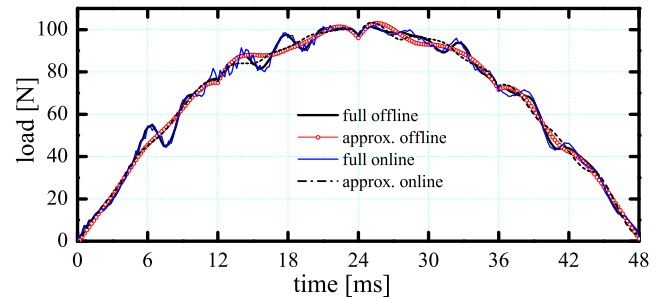


Fig. 6 Reconstructed moving load in the four considered cases (off-line full matrix, off-line approximated, online full matrix and online approximated)

shown in Figure 6. Note that although the identified loads have some obvious oscillations because of the noise contamination, they could be reconstructed with good accuracy, partly thanks to the proper level of singular value truncation of the system matrix. Approximation of the loads and the damage-related distortions by the load shape functions, besides reducing the numerical costs, helps to filter the noise to a certain degree while preserving the accuracy.

5.3.2 Damage identification

For each of the damaged elements, the best-fitting extents of the damages of both types (μ_α^{csr} and μ_α^{bc}) have been computed by (11) and used to identify the damage type by choosing the smaller fit value of (12). The results are listed in Tables 2, 3 and 4. Figure 7 plots the actual, raw identified and fitted stress-strain relationships.

In general, the damage type could be properly identified by choosing the one that fits the stress-strain relationship better, i.e. minimizes the fit (12). However, in online

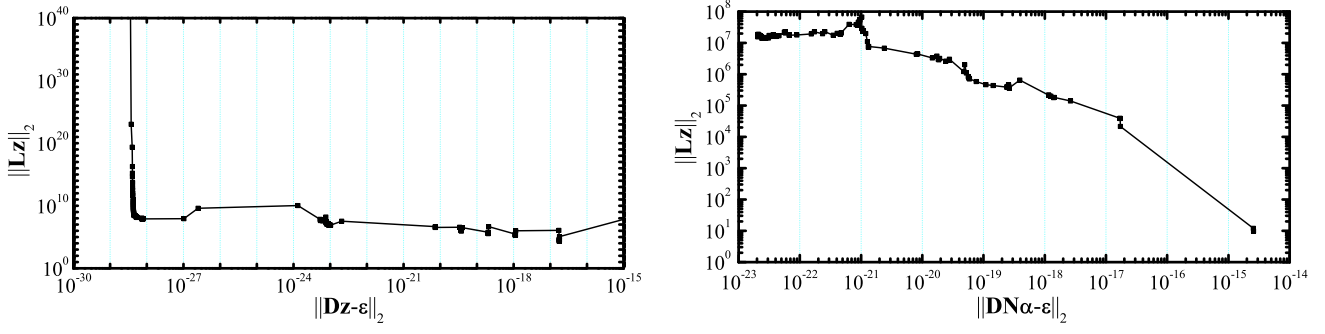


Fig. 4 L-curve (norm of the first differences vs. the residual, L is the matrix of the first differences), off-line identification: (left) full matrix; (right) approximated matrix

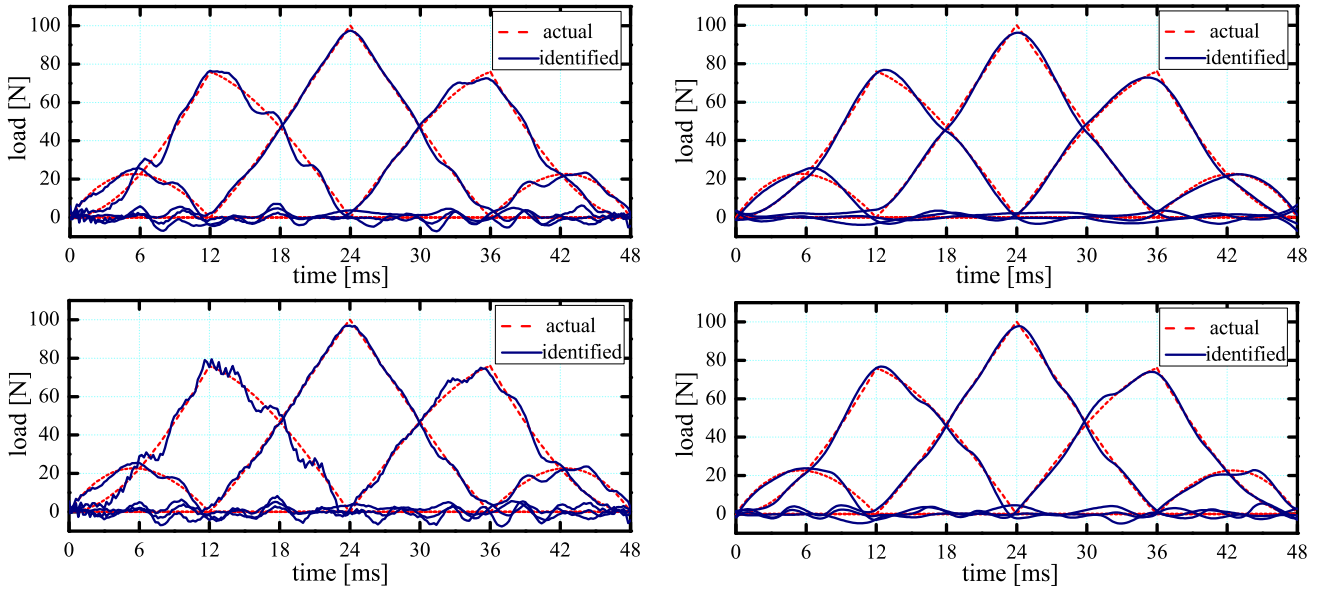


Fig. 5 Identified equivalent nodal loads: (top left) off-line, full matrix (no approximations); (top right) off-line, approximated; (bottom left) online, full matrix (no approximations); (bottom right) online, approximated

Table 3 Online (full matrix) identification of damage extent (11) and damage type (by smaller fit (12)) for elements no. 21 and 32. Column “tension” lists the percentage of the time steps in tension

time section I			time section II			time section III			mean value	actual value
extent	fit (12)	tension	extent	fit (12)	tension	extent	fit (12)	tension		
$\mu_{21}^{csr}=0.6514$	0.1351	70.0%	$\mu_{21}^{csr}=0.9468$	0.0273	20.8%	$\mu_{21}^{csr}=0.9980$	0.0049	10.8%	—	—
$\mu_{21}^{bc}=0.5964$	0.0343		$\mu_{21}^{bc}=0.5826$	0.0064		$\mu_{21}^{bc}=0.4086$	0.0048		$\mu_{21}^{bc}=0.529$	$\mu_{21}^{bc}=0.6$
$\mu_{32}^{csr}=0.2814$	0.1547	89.2%	$\mu_{32}^{csr}=0.2726$	0.0354	85.8%	$\mu_{32}^{csr}=0.2657$	0.0866	38.3%	$\mu_{32}^{csr}=0.273$	$\mu_{32}^{csr}=0.3$
$\mu_{32}^{bc}=0.2851$	0.1627		$\mu_{32}^{bc}=0.2725$	0.0399		$\mu_{32}^{bc}=0.2507$	0.7394		—	—

Table 4 Online approximated identification of damage extent (11) and damage type (by smaller fit (12)) for elements no. 21 and 32. Column “tension” lists the percentage of the time steps in tension

time section I			time section II			time section III			mean value	actual value
extent	fit (12)	tension	extent	fit (12)	tension	extent	fit (12)	tension		
$\mu_{21}^{csr}=0.7323$	0.0699	70.8%	$\mu_{21}^{csr}=0.9530$	0.0203	21.7%	$\mu_{21}^{csr}=0.9992$	0.0014	12.5%	—	—
$\mu_{21}^{bc}=0.5965$	0.0019		$\mu_{21}^{bc}=0.5928$	0.0007		$\mu_{21}^{bc}=0.5009$	0.0013		$\mu_{21}^{bc}=0.563$	$\mu_{21}^{bc}=0.6$
$\mu_{32}^{csr}=0.2821$	0.0114	95.0%	$\mu_{32}^{csr}=0.2721$	0.0179	85.0%	$\mu_{32}^{csr}=0.2750$	0.0709	41.7%	$\mu_{32}^{csr}=0.276$	$\mu_{32}^{csr}=0.3$
$\mu_{32}^{bc}=0.2821$	0.0118		$\mu_{32}^{bc}=0.2706$	0.0875		$\mu_{32}^{bc}=0.2558$	0.5318		—	—

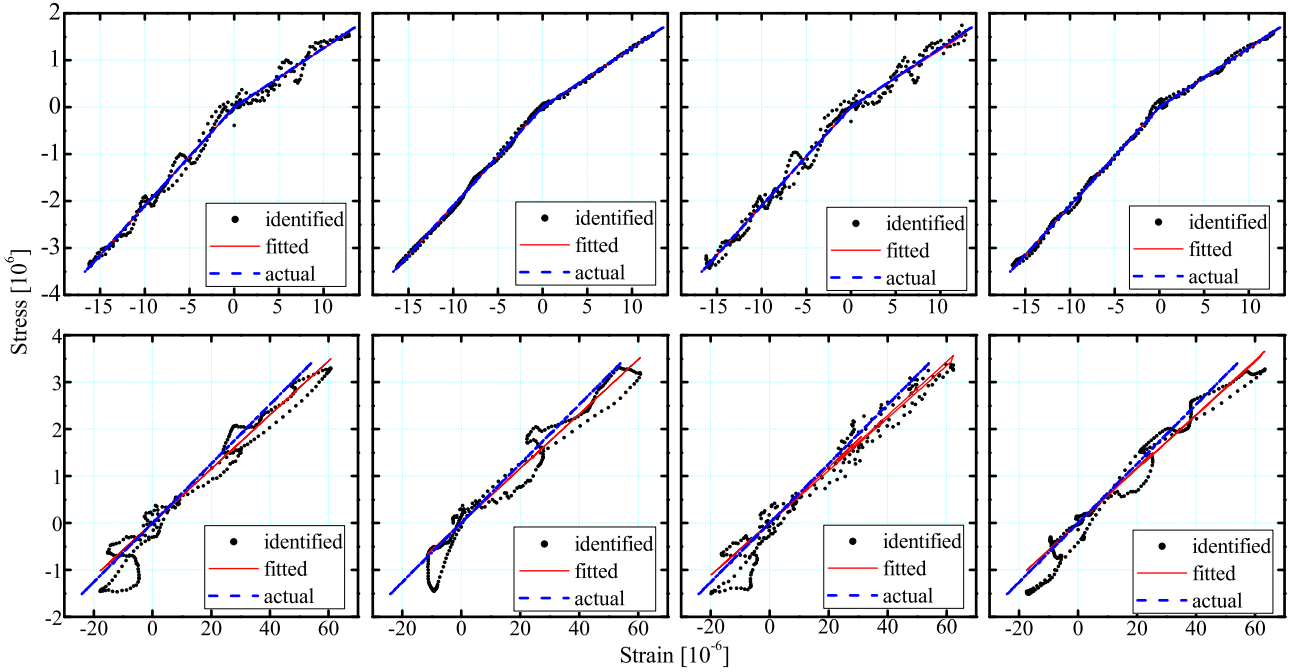


Fig. 7 Actual, raw identified and fitted stress-strain relationships for elements no. 21 (breathing crack, first row) and 32 (constant stiffness reduction, second row): (first column) off-line, full matrix; (second column) off-line approximated; (third column) online, full matrix; (fourth column) online approximated

Table 2 Off-line identification of damage extent (11) and damage type (by smaller fit (12)) for elements no. 21 and 32

full matrix		approximated		actual value
extent	fit (12)	extent	fit (12)	
$\mu_{21}^{\text{SR}}=0.9046$	0.0424	$\mu_{21}^{\text{SR}}=0.9048$	0.0363	—
$\mu_{21}^{\text{bc}}=0.5950$	0.0068	$\mu_{21}^{\text{bc}}=0.5972$	0.0008	$\mu_{21}^{\text{bc}}=0.6$
$\mu_{32}^{\text{SR}}=0.2741$	0.0360	$\mu_{32}^{\text{SR}}=0.2765$	0.0464	$\mu_{32}^{\text{SR}}=0.3$
$\mu_{32}^{\text{bc}}=0.2699$	0.2480	$\mu_{32}^{\text{bc}}=0.2706$	0.1247	—

identification with short time sections, a damaged element may happen to be almost only in tension during a whole time section (as e.g. element no. 32 in time section I). In such a case the damage type cannot be reliably estimated in that specific section, since for distinguishing between both tested damage types compression data are necessary. Similarly, if an element with a damage of a breathing crack type is in compression almost the whole time section (as element no. 21 in time section III), a reliable differentiation between a marginal reduction of stiffness and a breathing crack is impossible. Nevertheless, these shortcomings are unavoidable; the proper damage type in such cases can be inferred only from the identification results in successive time sections.

Because of the noise influence, the recovered strain-stress relationships of the damaged elements take the form of a set of discrete points which are scattered around the actual relationships (Figure 7). The damage extents can be estimated

by least-square fitting. It should be noted that the identification accuracy varies a little between the time sections in the online identification case due to random Gaussian measurement error. However, all the tested identification schemes (off-line and online, with and without approximations) have yielded satisfactory results, which is especially important provided the considerably smaller numerical cost (by two to three orders of magnitude) of the online approximated method.

6 Conclusions

This paper proposes an effective methodology for identification of coexistent loads and damages, including damage types and extents. A practical long-term objective is monitoring of critical and impact loads for applications in forensic engineering and in Adaptive Impact Absorption systems (AIA) (Wikło and Holnicki-Szulc 2009b).

The methodology is based on the Virtual Distortion Method (VDM) and identifies damages of an arbitrary type via the recovered stress-strain relationships of the damaged elements. The method is applicable both off-line and online by a moving time window. The numerical costs can be considerably reduced by approximating the unknown loads and damage-related distortions with load shape functions.

A drawback of the method is the necessity of an a priori information on the locations of the loads and the damages

in order to keep the number of sensors reasonably small. In practical applications this information can be partly provided by a dedicated external system, e.g. ELGRID (Kokot and Holnicki-Szulc 2005). However, in the further research this drawback is also going to be addressed directly.

Acknowledgements The authors gratefully acknowledge the support of the Foundation for Polish Science through TEAM Programme 'Smart and Safe', co-financed by the EU European Regional Development Fund. This research is partially supported by the China National Natural Science Foundation under grant # 50579008.

References

- Adams R, Doyle JF (2002) Multiple force identification for complex structures. *Experimental Mechanics* 42(1):25–36
- Akgün MA, Garcelon JH, Haftka RT (2001) Fast exact linear and non-linear structural reanalysis and the Sherman-Morrison-Woodbury formulas. *International Journal for Numerical Methods in Engineering* 50(7):1587–1606
- Allen MS, Carne TG (2006) Comparison of inverse structural filter (ISF) and sum of weighted accelerations technique (SWAT) time domain force identification methods. In: 47th AIAA/ASME/ASCE/AHS/ASC Structures, Structural Dynamics, and Materials Conference
- Allen MS, Carne TG (2008) Delayed, multi-step inverse structural filter for robust force identification. *Mechanical Systems and Signal Processing* 22:1036–1054
- Briggs JC, Tse MK (1992) Impact force identification using extracted modal parameters and pattern matching. *International Journal of Impact Engineering* 12(3):361–372
- Cao X, Sugiyamac Y, Mitsui Y (1998) Application of artificial neural networks to load identification. *Computers and Structures* 69:63–78
- Dahlquist G, Björck Å (2008) *Numerical Methods in Scientific Computing*, vol II. to be published by SIAM, URL <http://www.mai.liu.se/~akbjo/NMbook.html>
- Doebbling SW, Farrar CR, Prime MB (1998) A summary review of vibration-based damage identification methods. *The Shock and Vibration Digest* 30(2):91–105
- Doyle JF (1997) A wavelet deconvolution method for impact force identification. *Experimental mechanics* 37(4):403–408
- Friswell MI, Penny JET (2002) Crack modeling for structural health monitoring. *Structural Health Monitoring* 1(2):139–148
- Ha QP, Trinh H (2004) State and input simultaneous estimation for a class of nonlinear systems. *Automatica* 40:1779–1785
- Hansen PC (2002) Deconvolution and regularization with Toeplitz matrices. *Numerical Algorithms* 29:323–378
- Holnicki-Szulc J (ed) (2008) *Smart Technologies for Safety Engineering*. John Wiley & Sons Ltd, Chichester
- Holnicki-Szulc J, Gierliński J (1995) *Structural Analysis, Design and Control by the Virtual Distortion Method*. Wiley, Chichester 1995. John Wiley & Sons Ltd, Chichester
- Inoue H, Ishida H, Kishimoto K, Shibuya T (1991) Measurement of impact load by using an inverse analysis technique: Comparison of methods for estimating the transfer function and its application to the instrumented Charpy impact test. *Japan Society of Mechanical Engineers International Journal* 34(4):453–458
- Inoue H, Harrigan JJ, Reid SR (2001) Review of inverse analysis for indirect measurement of impact force. *Applied Mechanics Reviews* 54(6):503–524
- Jacquelin E, Bennani A, Hamelin P (2003) Force reconstruction: analysis and regularization of a deconvolution problem. *Journal of Sound and Vibration* 265(1):81–107
- Jankowski Ł (2009) Off-line identification of dynamic loads. *Structural and Multidisciplinary Optimization* 37(6):609–623, DOI 10.1007/s00158-008-0249-0
- Klinkov M, Fritzen CP (2006) Online estimation of external loads from dynamic measurements. In: *Proceedings of the International Conference on Noise and Vibration Engineering (ISMA)*, Leuven, Belgium, pp 3957–3968
- Kokot M, Holnicki-Szulc J (2005) Health monitoring of electric circuits. *Key Engineering Materials* 293–294:669–676
- Kořakowski P, Mujica LE, Vehí J (2006) Two approaches to structural damage identification: Model updating vs. soft computing. *Journal of Intelligent Material Systems and Structures* 17(1):63–79
- Kořakowski P, Wikło M, Holnicki-Szulc J (2008) The virtual distortion method — a versatile reanalysis tool for structures and systems. *Structural and Multidisciplinary Optimization* 36(3):217–234, DOI 10.1007/s00158-007-0158-7
- Kress R (1989) *Linear integral equations*, Applied Mathematical Sciences, vol 82. Springer, New York
- Liu JJ, Ma CK, Kung IC, Lin DC (2000) Input force estimation of a cantilever plate by using a system identification technique. *Computer Methods in Applied Mechanics and Engineering* 190:1309–1322
- Ma CK, Ho CC (2004) An inverse method for the estimation of input forces acting on non-linear structural systems. *Journal of Sound and Vibration* 275:953–971
- Mujica LE, Vehí J, Rodellar J, Kořakowski P (2005) A hybrid approach of knowledge-based reasoning for structural assessment. *Smart Materials and Structures* 14:1554–1562
- Mujica LE, Vehí J, Staszewski W, Worden K (2006) Impact damage detection in aircraft composites using knowledge-based reasoning. In: *Proceeding of the 3rd European Workshop on Structural Health Monitoring*, Granada, Spain, pp 601–608
- Nair KK, Kiremidjian AS, Law KH (2006) Time series-based damage detection and localization algorithm with application to the ASCE benchmark structure. *Journal of Sound and Vibration* 291(1–2):349–368
- Nocedal J, Wright S (1999) *Numerical Optimization*. Springer Series in Operations Research, Springer, New York
- Ödeen S, Lundberg B (1991) Prediction of impact force by impulse responses method. *International Journal of Impact Engineering* 11(2):149–158
- Putresza JT, Kořakowski P (2001) Sensitivity analysis of frame structures — Virtual Distortion Method approach. *International Journal for Numerical Methods in Engineering* 50(6):1307–1329
- Silva S, Dias Júnior M, Lopes Jr V (2008) Structural Health Monitoring in Smart Structures Through Time Series Analysis. *Structural Health Monitoring* 7(3):231–244
- Staszewski WJ (2003) *Advances in Smart Technologies in Structural Engineering*, Springer, chap *Structural Health Monitoring using Guided Ultrasonic Waves*, pp 117–162
- Suwała G, Jankowski Ł (2008) A model-less method for impact mass identification. In: *Proceedings of the 4th European Workshop on Structural Health Monitoring*, Kraków, Poland, pp 365–373
- Uhl T (2007) The inverse identification problem and its technical application. *Archive of Applied Mechanics* 77(5):325–337
- Wei Z, Yam LH, Cheng L (2005) NARMAX model representation and its application to damage detection for multi-layer composites. *Composite Structures* 68(1):109–117
- Wikło M, Holnicki-Szulc J (2009a) Optimal design of adaptive structures. Part I. Remodeling for impact reception. *Structural and Multidisciplinary Optimization* 37(3):305–318, DOI 10.1007/s00158-008-0233-8

-
- Wikło M, Holnicki-Szulc J (2009b) Optimal design of adaptive structures. Part II. Adaptation to impact loads. *Structural and Multidisciplinary Optimization* 37(4):351–366, DOI 10.1007/s00158-008-0242-7
- Yan G (2006) Structural damage identification methods based on generalized flexibility matrix and wavelet analysis. PhD thesis, School of Civil Engineering, Harbin Institute of Technology, China
- Zhang Q, Jankowski Ł, Duan Z (2008) Identification of coexistent load and damage based on virtual distortion method. In: *Proceedings of the 4th European Workshop on Structural Health Monitoring*, Kraków, Poland, pp 1121–1128